

Thermal conduction in molecular chains: Non-Markovian effects

Dvira Segal^{a)}Chemical Physics Theory Group, Department of Chemistry, University of Toronto,
80 St. George Street, Toronto, Ontario M5S 3H6, Canada

(Received 11 February 2008; accepted 7 May 2008; published online 13 June 2008)

We study the effect of non-Markovian reservoirs on the heat conduction properties of short to intermediate size molecular chains. Using classical molecular dynamics simulations, we show that the distance dependence of the heat current is determined not only by the molecular properties, rather it is also critically influenced by the spectral properties of the heat baths, for both harmonic and anharmonic molecular chains. For highly correlated reservoirs the current of an anharmonic chain may exceed the flux of the corresponding harmonic system. Our numerical results are accompanied by a simple single-mode heat conduction model that can capture the intricate distance dependence obtained numerically. © 2008 American Institute of Physics.

[DOI: [10.1063/1.2938092](https://doi.org/10.1063/1.2938092)]

I. INTRODUCTION

The problem of heat conduction through molecular structures has recently attracted a lot of attention^{1–6} with potential applications in thermal machinery,^{7,8} information processing and computation,^{9,10} and thermoelectricity.^{11,12}

One of the major open questions here is what are the factors that dominate thermal transport, the molecular structure, the contacts, or both?³ Another central issue is the determination of the system size (N) dependence of the heat current J . While Fourier's law suggests the relation $J \propto N^{-1}$, extensive studies of heat flow in low dimensional systems have resolved a $J \propto N^{-\alpha}$ behavior, where α usually deviates from 1.¹³ Specifically, for periodic harmonic chains one gets $\alpha=0$ in the Markovian limit,¹⁴ i.e., the heat current does not depend on system size. This ballistic behavior results from the lack of scattering mechanisms between normal modes. In the harmonic limit the heat current thus reflects the spectral properties of the thermal reservoirs. In other words, it crucially depends on the details of the boundary conditions.^{15,16} In contrast, in strongly anharmonic systems where local thermal equilibrium exists, one expects that the steady state energy current will not depend on the properties of the contacts.

It should be emphasized, however, that Fourier's law is not generally fulfilled in one dimensional (1D) systems, even in the presence of nonlinear interactions, and/or molecular disorder.¹³ Extensive numerical simulations have manifested deviations from this diffusional law for both ordered and disordered chains showing, e.g., a soliton-type propagation.¹⁷

Recent studies of heat transport in disordered low-dimensional harmonic chains have exposed the influential role of the contacts' spectral properties on the asymptotic α value.^{15,18} Subsequent works exemplified this effect within anharmonic lattices.^{19,20} While these works have typically

focused on the asymptotic length behavior, our objective here is to systematically study the effect of the reservoirs' spectral properties on the thermal transport in *short to intermediate* size molecular junctions that are of experimental relevance.

Using classical molecular dynamics simulations, we analyze the thermal transport properties of periodic 1D chains. We study the distance dependence of the current and the chain's temperature profile for Markovian and non-Markovian thermal baths considering either harmonic or anharmonic internal molecular interactions. We find that the spectral properties of the reservoirs play a crucial role in determining the size dependence of the thermal current. Thus, one should carefully interpret experimental results,³ as both molecular structure and the properties of the boundaries critically determine the junction conductivity. Another interesting finding is that for highly correlated noise, anharmonic chains conduct more effectively than the corresponding harmonic systems. We qualitatively explain our numerical results using a single-mode heat conduction model that can be analytically solved.^{21,22}

II. MOLECULAR DYNAMICS SIMULATIONS

We present here detailed classical molecular dynamics simulations of steady state heat transfer through 1D periodic molecular chains coupled to non-Markovian reservoirs. We model the molecule as a chain of N identical atoms. The end particles 1 and N are connected to heat baths of temperatures T_L and T_R , respectively. The dynamics is governed by the generalized Langevin equation,

$$\begin{aligned} \ddot{x}_k(t) &= -\frac{1}{m} \frac{\partial H_0}{\partial x_k}, \quad k = 2, 3, \dots, N-1, \\ \ddot{x}_1(t) &= -\frac{1}{m} \frac{\partial H_0}{\partial x_1} - \int_0^t dt' \gamma_L(t-t') \dot{x}_1(t') + \eta_L(t), \end{aligned} \quad (1)$$

^{a)}Electronic mail: dsegal@chem.utoronto.ca.

$$\ddot{x}_N(t) = -\frac{1}{m} \frac{\partial H_0}{\partial x_N} - \int_0^t dt' \gamma_R(t-t') \dot{x}_N(t') + \eta_R(t),$$

where x_k is the position of the k particle of mass m , and p_k [see Eq. (5)] is the particle momentum. H_0 is the internal molecular Hamiltonian. γ_L and γ_R are friction constants and η_L and η_R are fluctuating forces that represent the effect of the thermal reservoirs. These terms are related through the fluctuation-dissipation relation ($n=L,R$),

$$\langle \eta_n \rangle = 0; \quad \langle \eta_n(t) \eta_n(t') \rangle = \frac{k_B T_n}{m} \gamma_n(t-t'), \quad (2)$$

where k_B is the Boltzmann constant. We consider here an exponentially correlated Ornstein–Uhlenbeck (O-U) noise,²³

$$\gamma_n(t-t') = \frac{\epsilon_n}{\tau_c^n} e^{-|t-t'|/\tau_c^n}, \quad (3)$$

with the intensity ϵ and a correlation time τ_c . For short correlation times the heat baths generate an uncorrelated (white) noise $\gamma_n(t-t') \xrightarrow{\tau_c^n \rightarrow 0} 2\epsilon_n \delta(t-t')$. The Fourier transform of the O-U correlation function, to be used below, is

$$\gamma_n(\omega) \equiv \int e^{-i\omega t} \gamma_n(t) dt = \frac{2\epsilon_n}{1 + (\omega \tau_c^n)^2}. \quad (4)$$

A simple approach for implementing the O-U noise in numerical simulations is to introduce auxiliary dynamical variables $y_1(t)$ and $y_N(t)$ for the L and R baths, respectively.²⁴ The new equations of motion for the first particle are

$$\begin{aligned} \dot{x}_1(t) &= \frac{p_1(t)}{m}, \\ \ddot{x}_1(t) &= -\frac{1}{m} \frac{\partial H_0}{\partial x_1} - y_1(t) + \eta_L(t), \\ \dot{y}_1(t) &= -\frac{y_1(t)}{\tau_c^L} + \frac{\epsilon_L}{m \tau_c^L} p_1(t), \\ \dot{\eta}_L(t) &= -\frac{\eta_L(t)}{\tau_c^L} + \frac{1}{\tau_c^L} \sqrt{\frac{2\epsilon_L k_B T_L}{m}} \mu_L(t), \end{aligned} \quad (5)$$

where $\mu_L(t)$ is a Gaussian white noise, $\langle \mu_L(t) \rangle = 0$, and $\langle \mu_L(t) \mu_L(t') \rangle = \delta(t-t')$. An equivalent set of equations exists for the N particle, interacting with the R thermal bath. The coupled equations [Eq. (1) for particles $2 \cdots N-1$ and Eq. (5) with its N equivalent] are integrated using the fourth order Runge–Kutta method to yield the positions and velocities of all particles. The heat flux can be calculated from the trajectory using¹³

$$J = \frac{1}{2(N-1)} \sum_{k=1}^{N-1} \langle (v_k + v_{k+1}) F(x_{k+1} - x_k) \rangle, \quad (6)$$

where $F(r) = -\partial H_0(r)/\partial r$, $v_k = p_k/m$, and we average over time after steady state is achieved.

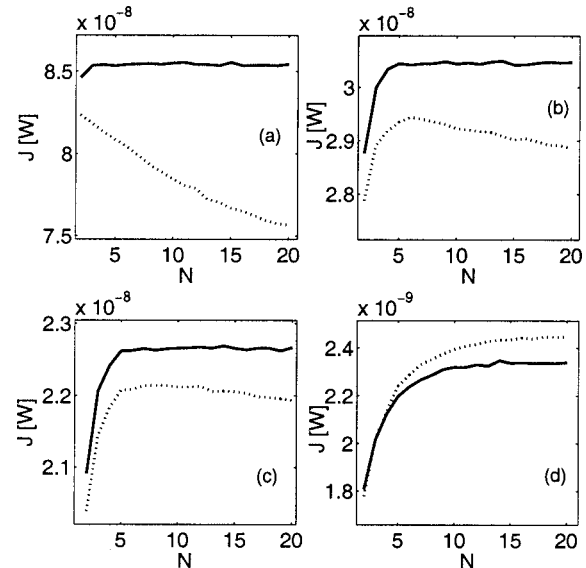


FIG. 1. Distance dependence of the heat current in non-Markovian systems for harmonic (full), and anharmonic (dotted) models. (a) Gaussian white noise, (b) O-U noise with $\tau_c = 8 \times 10^{-3}$ ps, (c) O-U noise with $\tau_c = 0.01$ ps, and (d) O-U noise with $\tau_c = 0.04$ ps. $T_R = 300$ K, $T_L = 0$ K, and $\epsilon = 50$ ps⁻¹ in all cases.

We describe next the molecular structure of the chain. We model the interactions between the atoms using a Morse potential of dissociation energy D , width α , and an interatomic equilibrium separation x_{eq} ,

$$H_0 = \sum_{k=1}^N \frac{p_k^2}{2m} + D \sum_{k=0}^N [e^{-\alpha(x_{k+1}-x_k-x_{eq})} - 1]^2. \quad (7)$$

The atoms indexed by 0 and $N+1$ are the left and right reservoirs atoms. We consider two sets of parameters: In the first case the potential width is taken to be very small $\alpha \ll 1$, so as the potential energy is practically harmonic with a force constant $2D\alpha^2$. We refer to this model as “harmonic.” We also use parameters where the anharmonic coefficient is large, α/\sqrt{mD} of order 1. We refer to the later case as “anharmonic.”

Unless otherwise stated, in the numerical simulation presented below we have typically used the following parameters: $D = 367.8/\nu^2$ kJ/mol, $\alpha = 1.875\nu$ Å⁻¹, $x_{eq} = 1.54$ Å, and $m = 12$ g/mol. These numbers describe a *c-c* stretching mode for $\nu = 1$.²⁵ We take $\nu = 0.01$ for the harmonic model, while in the anharmonic case we use $\nu = 6$. We also assume that the two reservoirs have the same type of spectral function (O-U) with equal strength $\epsilon = \epsilon_n$ and noise correlation time $\tau_c = \tau_c^n$. Depending on the situation, we have used integration time step $\Delta t = 10^{-3} - 10^{-4}(1/\omega)$, where ω is the molecular frequency in the harmonic limit. We also take care of the required inequality $\Delta t \ll \tau_c$.

Figure 1 presents the heat current for harmonic (J_H) and anharmonic (J_A) chains calculated with different memory times τ_c . Panel (a) shows the heat current in the Markovian limit. We find that the energy flux in harmonic systems does not depend on size, while it decays with distance for anharmonic chains in agreement with standard results¹³ [see Fig. 2(c) for a closer analysis]. When the noise correlation time is

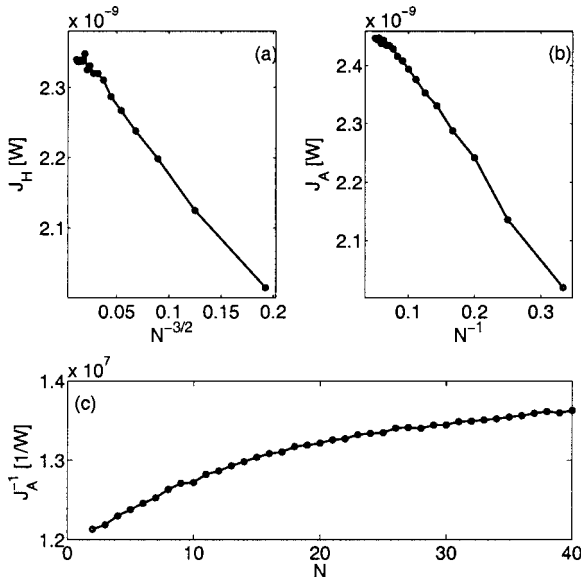


FIG. 2. Resolving the distance dependence of the thermal current in non-Markovian O-U systems for harmonic (a) and anharmonic (b) models, with $\tau_c=0.04$ ps, $T_R=300$ K, $T_L=0$ K, and $\epsilon=50$ ps $^{-1}$. (c) The thermal current for Markovian anharmonic chains with the parameters of Fig. 1(a), illustrating that Fourier's law is not satisfied in this model.

increased, an interesting behavior is observed [panel (b)]: While J_H shows an initial increase for $N < 5$, then remains a constant to a good approximation, the anharmonic flux initial rise is followed by a decay for long enough chains. As the memory time is further increased (c), the current of an anharmonic system saturates, and is approximately a constant over the relevant sizes. This observation interestingly shows a counteracting effect between the molecular contribution to the heat current and the reservoirs spectral properties. For highly correlated reservoirs (d) both harmonic and anharmonic currents are slightly enhanced with distance. Surprisingly, in this case the anharmonic junction conducts better than a fully harmonic system.

This intricate behavior sustains for a broad range of parameters. Figure 5 manifests that the current scales linearly with the temperature difference. Figure 6 further demonstrates that for weak system-bath couplings $J \propto \epsilon$.

We explain next these observations. First we clarify why J_H and J_A for short chains increase with N for non-Markovian baths. As was shown in Ref. 26 the dominant heat conducting vibrational modes of alkane chains are shifted towards lower frequencies with increasing molecular size. Since within the O-U model $\gamma(\omega)$ (reflecting the system-bath coupling) is larger at lower frequencies, the current gets enhanced with distance.

Next we explain the intricate current-distance behavior of anharmonic systems. Anharmonic interactions lead to scattering processes between the molecular modes. These scattering effects are more influential with increasing chain length. In Markovian systems this results in the enhancement of the junction resistance, thus it leads to the reduction of current with N . However, in non-Markovian systems these scattering effects are actually beneficial for transferring energy from molecular modes which are above the reservoirs' cut-off frequencies, into low energy modes that overlap with

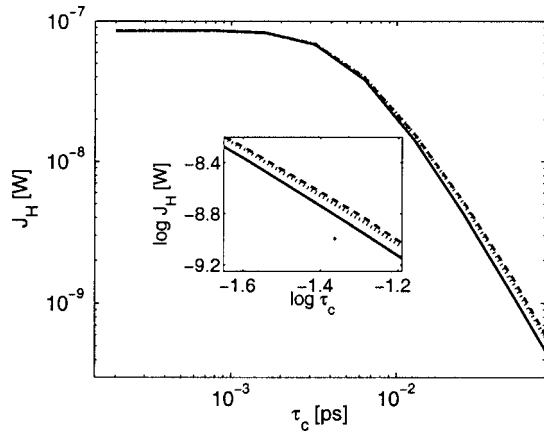


FIG. 3. Decrease of heat current with increasing bath correlation time for harmonic systems. $T_R=300$ K, $T_L=0$ K, and $\epsilon=50$ ps $^{-1}$. $N=2$ (full), $N=5$ (dotted), and $N=10$ (dashed). The inset zooms on the high τ_c values.

the solids vibrations. The interplay between these two effects leads to a rich behavior: If τ_c^{-1} is higher than the molecular frequencies, here of the order of 150 ps $^{-1}$, anharmonic effects lead to the reduction of current with size [see panels (a) and (b)]. In the opposite small cutoff limit (d), $\tau_c^{-1}=25$ (1/ps), harmonic systems can transfer only those modes that are in the reservoirs energy window, while anharmonic junctions better conduct by scattering high energy modes into low frequencies. For $\tau_c \sim 0.01$ ps the two effects practically cancel and J_A weakly depends on distance (c).

Figures 2(a) and 2(b) present the distance dependence of the energy flux for both harmonic and anharmonic chains assuming solids of long memory time $\tau_c=0.04$ ps. While it is difficult to make a definite conclusion, we find that J_H and J_A obey different functional forms. We also study [panel (c)] the distance dependence of the current in the Markovian limit, plotting J_A^{-1} as a function of size. We find that Fourier's ($J \propto N^{-1}$) functional form is not obeyed in this model. This is another manifestation that in low-dimensional systems, even in the presence of strong nonlinear interactions, the diffusional dynamics does not generally set in.¹³

Next we systematically explore the dependence of the heat flux on the reservoirs' correlation time. Figures 3 and 4 manifest that the Markovian behavior sustains for times up to $\tau_c \sim 5 \times 10^{-3}$ ps. For longer correlation times the heat current significantly decays with τ_c for both harmonic and anharmonic chains. The inset of Fig. 4 further shows that for $\tau_c \sim 6 \times 10^{-3}$ ps the anharmonic heat flux is practically distance independent [see also Fig. 1(c)]. This time is indeed of the order of the inverse of characteristic molecular vibrations ~ 150 ps $^{-1}$. As discussed above, this intriguing behavior results from an effective cancellation between internal molecular interactions, leading to the decay of current with N , and the reservoirs properties, which can lead to an enhancement of current with distance. In the next section we present a simple analytical model that can capture this intricate behavior.

In Fig. 5 we study the temperature dependence of the heat current for both Markovian and non-Markovian chains for a representative length $N=8$. We find that both harmonic and anharmonic systems show a linear current-temperature

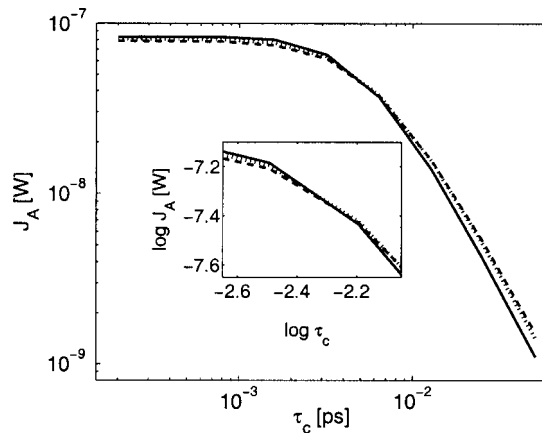


FIG. 4. Decrease of heat current with increasing bath correlation time for an anharmonic molecular model. $N=2$ (full), $N=5$ (dotted), and $N=10$ (dashed). $T_R=300$ K, $T_L=0$ K, and $\epsilon_n=50$ ps $^{-1}$. The inset zooms on intermediate τ_c values where J_A is independent of length.

relationship in the range of $T=0\text{--}300$ K. The thermal conductance ($J/\Delta T$) calculated from Figs. 1–4 is therefore approximately independent of temperature.

We have also analyzed in Fig. 6 the ϵ dependence of the current for Markovian and O-U systems, and found an approximate linear relation in the low dissipation regime. For Markovian baths the current decreases as ϵ^{-1} when the coupling is strong, $\epsilon>100$ ps $^{-1}$. We expect that the colored noise model will demonstrate a similar behavior for very strong molecule-bath interactions.²⁰

We conclude this section by noting that the qualitative behavior observed above (Figs. 1–4) applies for a broad range of temperatures and coupling parameters. We expect that similar characteristics will be discovered in molecular systems of various anharmonic internal interactions.

III. SINGLE-MODE HEAT CONDUCTION MODEL

We present here a simple model that yields a qualitative explanation for the influential role of non-Markovian reservoirs on the heat transfer properties of short to intermediate ($N=2\text{--}20$) molecular chains. In our minimal picture, heat current in a linear molecular system is dominated by a *specific* vibrational mode of frequency ω_0 .

This simplified picture neglects, of course, the detailed molecular properties, yet it contains two important elements that are crucial for understanding heat flow at the nanoscale: (i) Nonlinear effects might be included in the model by considering an anharmonic (truncated) molecular mode. (ii) Molecule-solid interactions and bath memory effects can be analyzed without being masked by the complicated molecular spectrum. An underlying assumption here is that energy transfer between modes is not significant for relatively short chains. Thus, studying the transfer of energy per mode is a reasonable description.

This elementary model is thus expected to be beneficial for identifying the imprint of the bath spectral properties on the junction thermal conduction. The model was also utilized for studying thermal rectification in molecular junctions, showing qualitative agreement with numerical simulations.²¹

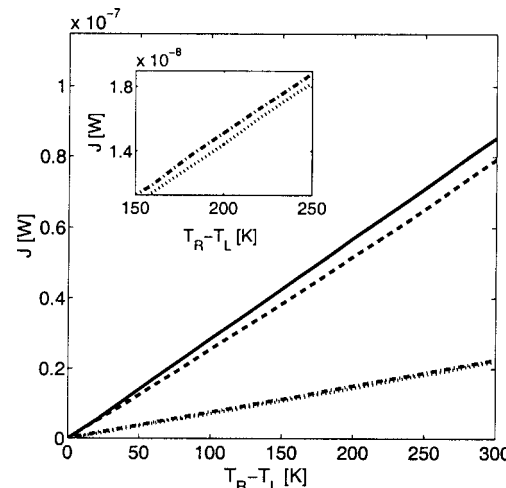


FIG. 5. Temperature dependence of the thermal flux, $N=8$, $T_R=300$ K. Harmonic chain with white noise (full), anharmonic chain with white noise (dashed), harmonic chain with O-U noise, $\tau_c=0.01$ ps, $\epsilon=50$ ps $^{-1}$ (dashed-dotted), and anharmonic chain with O-U noise, $\tau_c=0.01$ ps, $\epsilon=50$ ps $^{-1}$ (dotted). The inset zooms on the O-U simulations.

The total Hamiltonian of the simplified model includes three terms, $H=H_B+H_0+H_I$, where for a harmonic local mode,

$$\begin{aligned} H_B &= \sum_{j,n} \frac{p_{j,n}^2}{2m_j} + \frac{1}{2} m_j \omega_j^2 q_{j,n}^2, \\ H_0 &= \frac{p_0^2}{2M} + \frac{M \omega_0^2 q_0^2}{2}, \\ H_I &= \sum_{j,n} \lambda_{j,n} q_{j,n} q_0. \end{aligned} \quad (8)$$

H_B includes two thermal reservoirs $n=L,R$ of different temperatures, each consisting a set of independent harmonic oscillators with masses m_j , coordinates $q_{j,n}$, and momenta $p_{j,n}$. H_0 represents the (single) relevant molecular mode with coordinate q_0 , momentum p_0 , mass M , and frequency ω_0 . It can be written equivalently in the energy representation as $H_0=\sum_{l=0,1,2,\dots} l\omega_0|l\rangle\langle l|$; $\hbar=1$. If we sum over states up to infinity ($l\omega_0\gg T_n$), this term describes a harmonic mode as in Eq. (8). We can also model an anharmonic molecule by truncating the single mode spectrum to include only few vibrational states.^{21,22} The system-bath interaction is taken to be bilinear, with $\lambda_{j,n}$ as the coupling constant.

Assuming weak molecule-bath coupling at both ends, an analytical expression for the heat current in steady state can be derived using the master equation formalism.^{21,22} In the harmonic limit and at high temperatures ($T>\omega_0$) the thermal current is given by a Landauer type expression,²¹

$$J_H = \frac{\gamma_L(\omega_0)\gamma_R(\omega_0)}{\gamma_L(\omega_0)+\gamma_R(\omega_0)} k_B \Delta T, \quad (9)$$

where $\Delta T=T_R-T_L$ and $\gamma_n(\omega)=(\pi/2)\sum_j(\lambda_{j,n}^2/Mm_j\omega_j^2)\delta(\omega-\omega_j)$ is the Fourier transform of the friction constant $\gamma_n(t)$ (1).²⁷ The memory damping can be also expressed in terms of the reservoir's spectral function $g_n(\omega)=2\pi\sum_j(\lambda_{j,n}^2/Mm_j\omega_j)\delta(\omega-\omega_j)$ as $\gamma_n(\omega)=g_n(\omega)/4\omega$.

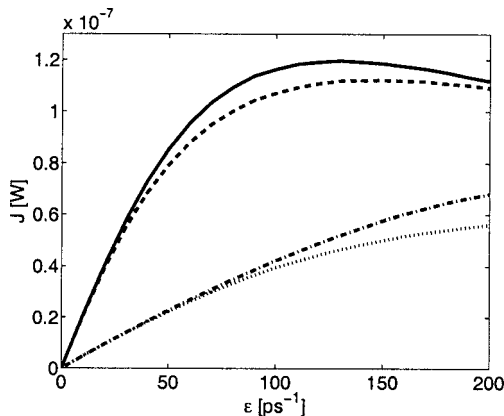


FIG. 6. Thermal flux as a function of system-bath coupling strength ϵ , $T_R = 300$ K, and $T_L = 0$ K. Parameters and lines setting are the same as in Fig. 5.

Equation (9) clearly manifests that in the harmonic limit the heat current is exclusively determined by the spectral properties of the reservoirs. This behavior results from the lack of scattering mechanisms in the harmonic system.

As mentioned above, within this simple picture we can also model a highly anharmonic molecule by truncating the single mode spectrum. For a two-level model ($l=0,1$) at high temperatures the heat current is given by²¹

$$J_A = \frac{\gamma_L(\omega_0)\gamma_R(\omega_0)}{\gamma_L(\omega_0) + \gamma_R(\omega_0)} \frac{\omega_0}{2T_B} \Delta T, \quad (10)$$

where the temperature of the local model (sometimes referred to as a bridge B) is

$$T_B = \frac{\gamma_L(\omega_0)T_L + \gamma_R(\omega_0)T_R}{\gamma_L(\omega_0) + \gamma_R(\omega_0)}. \quad (11)$$

Though expressions (9) and (10) provide the heat current for a simplistic single mode model, they may serve us for gaining qualitative understanding of heat transfer in an N -sites molecule. The key element here is the observation that in short linear chains relatively few modes contribute to the transport of thermal energy.²⁶ Using the usual harmonic dispersion law,²⁸ $\omega_k \propto |\sin \pi ka/N|$, k is an integer, and a is the lattice constant, we may assume for simplicity that a *single* long wavelength mode ($\pi ka \ll N$) dominates the dynamics, effectively coupled to both ends. We use the following generic form to describe its size dependence:

$$\omega_0 \approx \omega_M \left(1 + \frac{\beta}{N}\right). \quad (12)$$

ω_M is the asymptotic frequency for large N , and β is a constant that is specific for the material. Note that Eq. (12) does not necessarily describe the variation of the lowest vibrational mode of the chain with increasing length. Rather, this is a qualitative expression for the variation of the *dominant* heat conducting mode with size: For short chains the spectrum is significantly altered with size. For large enough chains ω_0 is approximately fixed.

We can clearly discern in Eqs. (9) and (10) the role of different factors (contacts and internal interactions) in determining the heat current. While the reservoirs spectral properties enter these expressions through the damping rate γ ,

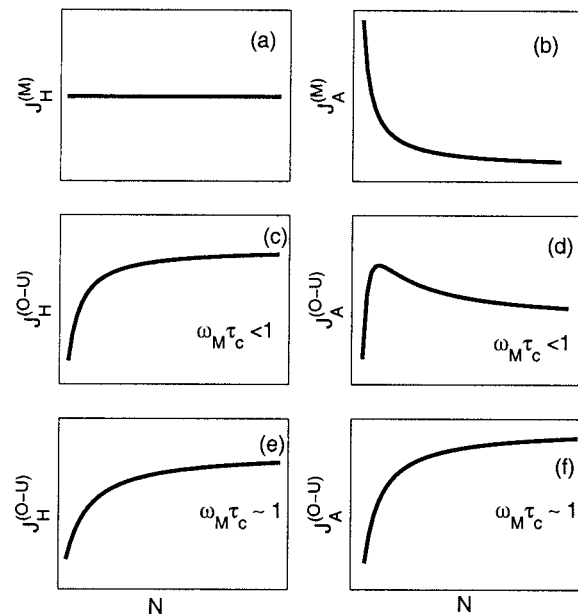


FIG. 7. Qualitative behavior of the heat current in the single-mode heat conduction model for Markovian and non-Markovian reservoirs. [(a) and (b)] Heat current for a Gaussian white noise [Eq. (13)]. [(c) and (d)] current for an O-U noise with a short memory time, Eq. (14) with $\omega_M\tau_c < 1$, and [(e) and (f)] current for an O-U noise with a long memory time, Eq. (14) with $\omega_M\tau_c \sim 1$.

calculated at the relevant molecular frequency ω_0 , anharmonic interactions yield an extra ω_0/T_B factor that accounts for the local mode occupancy. Since both of these terms depend on frequency, thus on size through Eq. (12), the resulting N dependence is not trivial. We study next various models for the damping element, namely, Markovian and non-Markovian, assuming for simplicity that the system is symmetric with respect to the two ends, $\gamma = \gamma_n$ ($n=L,R$).

A. Markovian process

For a Markovian process the spectral function is Ohmic, $g(\omega) = 4\epsilon\omega$, thus the friction is constant, $\gamma(\omega) = \epsilon$. In this limit Eqs. (9) and (10) reduce to

$$J_H^M = \frac{\epsilon}{2} k_B \Delta T, \quad (13)$$

$$J_A^M = \frac{\epsilon \Delta T \omega_M}{2(T_L + T_R)} \left(1 + \frac{\beta}{N}\right).$$

These expressions are consistent with standard results:¹³ The current in harmonic systems does not depend on size, while in anharmonic models it decays with distance. In Figs. 7(a) and 7(b) we qualitatively exemplify this behavior by simulating Eq. (13), reproducing the results of panel (a) of Fig. 1.

B. Ornstein–Uhlenbeck noise

The exponentially correlated (O-U) process $\gamma(t) = \epsilon/\tau_c e^{-|t|/\tau_c}$ transforms into a Lorentzian in frequency domain $\gamma(\omega) = 2\epsilon/(1 + \omega^2\tau_c^2)$. The fluxes (9) and (10) then become ($\epsilon = \epsilon_n$ and $\tau_c = \tau_c^n$),

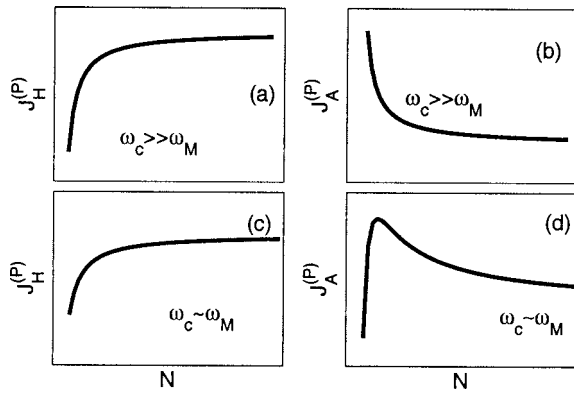


FIG. 8. Qualitative behavior of heat current in the single-mode heat conduction model with a power law spectral function (15), $s=1$.

$$\begin{aligned} J_H^{(O-U)} &= \frac{k_B \Delta T \epsilon}{1 + \omega_0^2 \tau_c^2} \propto \left(1 - \frac{\beta}{N}\right)^2, \\ J_A^{(O-U)} &= \frac{\Delta T}{T_L + T_R} \frac{\epsilon \omega_0}{1 + \omega_0^2 \tau_c^2} \propto \left(1 - \frac{\beta}{N}\right), \end{aligned} \quad (14)$$

where we derived the approximate distance dependence by assuming that $\omega_0 \tau_c > 1$ and taking $\beta/N < 1$. These expressions clearly demonstrate an *enhancement* of the current with N for both harmonic and anharmonic systems when the reservoirs have (each) a highly correlated noise.

In Figs. 7(c)–7(f) we simulate Eq. (14). For short correlation time we reproduce the results of Fig. 1(b), manifesting an enhancement of the anharmonic flux followed by a decrease of current. For very long correlation times the current systematically increases with size, in agreement with the numerical data [Fig. 1(d)].

C. Power law models

The spectral function $g(\omega) = \epsilon \omega^s e^{-\omega/\omega_c}$ is a widely accepted description of solids, where ω_c is the reservoir cutoff frequency. Unlike the O-U noise which satisfies the differential equation [Eq. (5)], this noise cannot be reduced into a multicomponent Markovian process, thus it is not trivial to simulate.²⁹ Within the single-mode heat conduction model the heat current for harmonic and anharmonic modes [Eqs. (9) and (10)] is given by

$$\begin{aligned} J_H^{(P)} &= \frac{\epsilon}{2} k_B \Delta T \omega_0^{s-1} e^{-\omega_0/\omega_c}, \\ J_A^{(P)} &= \epsilon \frac{\Delta T}{2(T_L + T_R)} \omega_0^s e^{-\omega_0/\omega_c}, \end{aligned} \quad (15)$$

where ω_0 is the dominant frequency for heat transport [Eq. (12)]. For an Ohmic ($s=1$) bath, taking $\omega_c \gg \omega_0$, the dynamics reduces to the Markovian limit [Eq. (13)], where $J_H^{(P)}$ is weakly enhanced with distance and $J_A^{(P)}$ decays with N . This behavior is exemplified in Figs. 8(a) and 8(b). In contrast, for $\omega_c \sim \omega_0$, a different trend is observed: While $J_H^{(P)}$ monotonically increases with length (c), in anharmonic systems the current first increases with size, then falls down (d). For

$s=2$ we expect that, quite interestingly, the heat current in harmonic models will *decay* with distance. This is because for long chains the dominant conducting frequencies are red shifted, while the solid spectral function is maximal at ω_c .

In conclusion, short to intermediate-size molecular chains coupled to general environments can manifest a rich behavior: The thermal current can either increase or decrease with size, critically depending both on the molecular internal interactions and on the reservoirs spectral properties. Despite its simplicity, the model presented here provides a useful starting point for explaining the complicated behavior observed within atomistic classical molecular dynamics simulations. In the next section we show that this model is also a useful tool for estimating the temperature profile along the conducting molecule.

IV. TEMPERATURE PROFILE

We investigate next the effect of the reservoir spectral properties on the local temperature profile in harmonic and anharmonic chains. Within the single-mode heat conduction model one can define in steady state the temperature of the local mode as $k_B T_B = \omega_0 \sum_l P_l$, where P_l is the population of the l vibrational state. In the classical limit it can be shown that this expression reduces to Eq. (11) [$T_B = \gamma_L(\omega_0) T_L + \gamma_R(\omega_0) T_R / \gamma_L(\omega_0) + \gamma_R(\omega_0)$] for both harmonic and anharmonic local modes.^{21,22} We therefore expect that when the reservoirs have the same type of spectral function with the same coefficients the temperature profile is independent of the type, and is given by the arithmetic average $T_B = (T_L + T_R)/2$. On the other hand, when the two reservoirs have different types of spectral densities (or different memory times), the temperature profile along the chain depends on the model. For example, if $T_L \ll T_R$ and $\gamma_R \ll \gamma_L$, $T_B \sim \gamma_R T_R / \gamma_L \ll T_R$. In contrast, for $T_L \ll T_R$ but $\gamma_R \gg \gamma_L$, $T_B \sim T_R$. This behavior was observed by Saito *et al.* in the harmonic limit using a quantum master equation formalism.¹⁶

Using classical molecular dynamics simulations we compute the temperature profile by calculating the mean kinetic energy for each particle $T_k = \langle p_k^2/m \rangle/k_B$. Here p_k is the momentum of the k th particle calculated after steady state develops, and we average over time and initial configurations using the procedure and parameters of Sec. II.

Figure 9 manifests that the bulk temperature profile is close to the arithmetic average (150 K) for both Markovian and non-Markovian systems when the reservoirs are identical. At the boundaries we see interesting features noted earlier in Refs. 14, 16, 30, and 31: The temperature close to the cold end (L) slightly rises, even to values higher than the average temperature. For an anharmonic system a small temperature gradient develops at the chain center. This effect is more pronounced for Markovian reservoirs. Note that in Markovian harmonic systems the temperature at the chain center, e.g., T_{10} , is higher than the anharmonic value. This trend is reversed for O-U baths, as here anharmonic interactions facilitate equilibration with the slow environment.

We employ next reservoirs of different spectral properties, and study the heat current and temperature profiles in

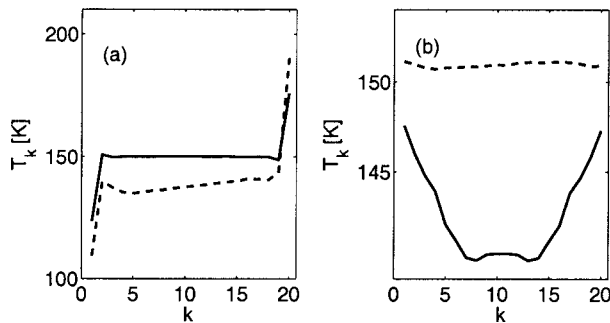


FIG. 9. Temperature profile along harmonic (full) and anharmonic (dashed) chains coupled to reservoirs of identical spectral properties. (a) Gaussian white noise and (b) O-U noise with $\tau_c=0.04$ ps. $N=20$, $T_R=300$ K, and $T_L=0$ K, and $\epsilon=50$ ps $^{-1}$ in all cases.

this asymmetric system. We assume that both reservoirs are of O-U type, but take different memory times $\tau_c^L \neq \tau_c^R$. Figure 10 manifests that the current in a harmonic system is independent of the direction of the asymmetry, i.e., if the cold bath is weakly or strongly coupled to the molecule. In contrast, the current in an anharmonic chain is significantly altered when the asymmetry is reversed: It is higher when the hot bath is slow. This response to spatial asymmetry is the underlying principle of the “thermal rectifier.”^{4,21,32}

Figure 11 shows that the bridge temperature dramatically responds to the direction of the asymmetry for *both harmonic and anharmonic systems*. We find that it is close to the temperature of the reservoir with the short memory time. In other words, the molecule better equilibrates with the Markovian reservoir. This behavior is consistent with the results of Ref. 16, and qualitatively agrees with Eq. (11).

V. DISCUSSION AND SUMMARY

In this paper we have investigated the effect of the contacts’ spectral properties on the thermal conduction of harmonic and anharmonic short to intermediate size periodic chains using classical molecular dynamics simulations. When the system size is smaller than the mean free path, heat conduction is dominated by harmonic interactions. In such

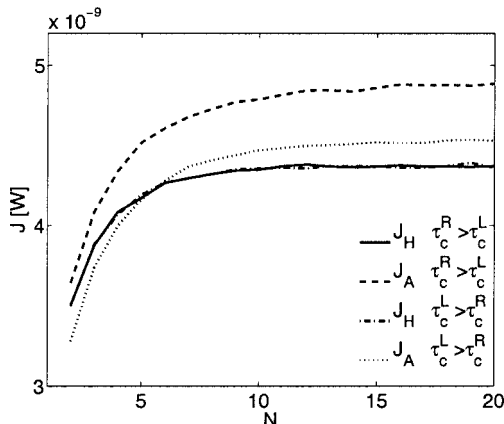


FIG. 10. Heat current in molecular chains coupled to reservoirs of different spectral properties $\tau_c^L \neq \tau_c^R$ and $\epsilon_L=\epsilon_R=50$ ps $^{-1}$. $\tau_c^L=0.002$ ps and $\tau_c^R=0.04$ ps: harmonic (full) and anharmonic (dashed). $\tau_c^L=0.04$ ps and $\tau_c^R=0.002$ ps: harmonic (dashed-dotted) and anharmonic (dotted). $T_R=300$ K and $T_L=0$ K in all cases.

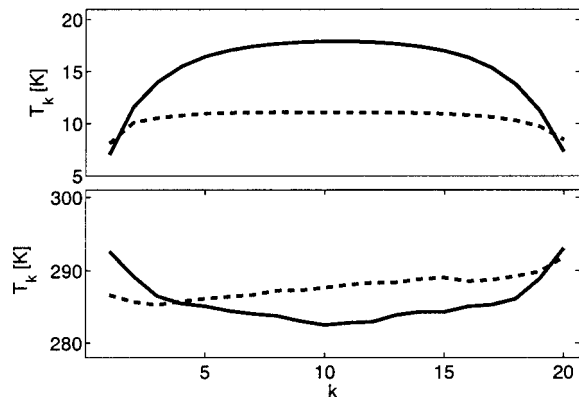


FIG. 11. Temperature profile along harmonic (full) and anharmonic (dashed) chains coupled to reservoirs of different spectral properties $\tau_c^L \neq \tau_c^R$ and $\epsilon_L=\epsilon_R=50$ ps $^{-1}$. $\tau_c^R=0.04$ ps, $\tau_c^L=0.002$ ps (top), $\tau_c^R=0.002$ ps, and $\tau_c^L=0.04$ ps (bottom). The temperature profile was calculated for an $N=20$ sites chain using $T_R=300$ K and $T_L=0$ K in all cases.

systems the spectral properties of the contacts play a central role in determining the dynamics in the junction.

This effect can be observed experimentally. The Debye temperature of standard crystals typically varies between 100 and 2000 K, translating into cutoff frequencies of 8–150 meV.²⁸ While the O-U spectral function employed here, $g(\omega)=4\pi\gamma(\omega)\propto\omega/1+\omega^2\tau_c^2$ does not comply with the standard Debye model $g(\omega)\propto\omega e^{-\omega/\omega_D}$, both functions show a maximum at the characteristic frequencies $1/\tau_c$ and ω_D , respectively, where ω_D is identified as the solid cutoff frequency, and τ_c is the bath correlation time in the O-U model. Thus, we can relate the inverse of the Debye frequency with the memory time of the O-U noise, $\omega_D \sim 1/\tau_c$. Based on our numerical results we therefore expect that the conduction properties of alkane chains confined between GaAs ($\omega_D^{-1}=0.13$ ps) or diamond solids ($\omega_D^{-1}=0.024$ ps) will significantly differ, by an order of magnitude, see, e.g., Figs. 3 and 4.

We also predict that the distance dependence of the current should strongly vary as a function of the bath (noise) correlation time: While for Markovian baths the current in harmonic systems is independent of size, it slightly increases with length when the reservoirs have long memory. The effect is even more dramatic in anharmonic chains. Here the current decays with N in the Markovian limit, while it gets enhanced with distance when the reservoirs have long memory times.

Other interesting observations are (i) we identified a regime where the anharmonic flux is practically distance independent due to the counteracting effects of molecular nonlinearities and bath correlations. (ii) For long memory times the current through anharmonic chains might be higher than the analogous harmonic current. Thus, anharmonic interactions might play a surprising role, enhancing the heat flux across molecules coupled to non-Markovian reservoirs. We also showed that the single-mode heat conduction model developed in Ref. 21 can essentially capture the length dependence and the temperature profile obtained within classical molecular dynamics simulations.

Before we conclude we briefly discuss the relationship

of our calculations to relevant experiments. Wang *et al.*³ have recently measured the thermal conductance ($\mathcal{K}=J/\mathcal{A}\Delta T$, where \mathcal{A} is the cross section) of 8–10 Au-alkandithiols monolayers-GaAs junctions. The values $\mathcal{K} \sim 25\text{--}28 \text{ MW m}^{-2} \text{ K}^{-1}$ were obtained, roughly independent of system size. Previous calculations²⁶ confirm this observation: The heat current of alkane chains is expected to be distance independent, even for very long ($N=100$) molecules, due to weak anharmonic internal interactions in the system. More qualitatively, using $\omega_D^{-1} \sim \tau_c \sim 0.13 \text{ ps}$ for GaAs and $\tau_c \sim 0.3 \text{ ps}$ for Au, assuming $\epsilon=50 \text{ ps}^{-1}$ and taking the surface density of molecules as $4.5 \times 10^{14} \text{ cm}^{-2}$,³³ we predict a thermal conductance of $\mathcal{K} \sim 10 \text{ MW m}^{-2} \text{ K}^{-1}$ (see Fig. 4). This number is only approximate, as the actual strength of the molecule-solid coupling is not known, the modeling of the hydrocarbon was restricted to the backbone structure, and the description of the reservoirs' spectral properties was reduced into a simple (O-U) form. Under these uncertainties, the conductance calculated here is in a reasonable agreement with the experimental results.

Several future directions are of interest. First, we have restricted our discussion to the O-U correlation function, since it could be easily simulated as a multicomponent Markovian process.²⁴ It is worth extending this study to include more realistic environments of ω^s spectral properties. These types of noise correlations can be simulated using the inverse Fourier transform technique.^{29,34,35} Other interesting questions are what is the role of the contacts in higher dimensions and how do quantum mechanical effects alter the phenomena addressed in this paper.^{16,26,30,31,36–38}

Understanding thermal transport in molecule-solid interfaces is important for molecular electronic applications.³⁹ It is also an imperative step in the endeavor for developing unique molecular level thermal devices.^{8–10}

ACKNOWLEDGMENTS

This work was supported by a University of Toronto Start-up Grant.

¹P. Kim, L. Shi, A. Majumdar, and P. L. McEuen, *Phys. Rev. Lett.* **87**, 215502 (2001).

²Z. Ge, D. G. Cahill, and P. V. Braun, *Phys. Rev. Lett.* **96**, 186101 (2006).

- ³R. Y. Wang, R. A. Segelman, and A. Majumdar, *Appl. Phys. Lett.* **89**, 173113 (2006).
- ⁴C. W. Chang, D. Okawa, A. Majumdar, and A. Zettl, *Science* **314**, 1121 (2006).
- ⁵Z. Wang, J. A. Carter, A. Lagutchev, Y. K. Koh, N.-H. Seong, D. G. Cahill, and D. D. Dlott, *Science* **317**, 787 (2007).
- ⁶C. Chiritescu, D. G. Cahill, N. Nguyen, D. Johnson, A. Bodapati, P. Kebinski, and P. Zschack, *Science* **315**, 351 (2007).
- ⁷C. W. Chang, D. Okawa, H. Garcia, T. D. Yuzvinsky, A. Majumdar, and A. Zettl, *Appl. Phys. Lett.* **90**, 193114 (2007).
- ⁸D. Segal and A. Nitzan, *Phys. Rev. E* **73**, 026109 (2006).
- ⁹L. Wang and B. Li, *Phys. Rev. Lett.* **99**, 177208 (2007).
- ¹⁰Z. Liu and B. Li, *Phys. Rev. E* **76**, 051118 (2007).
- ¹¹P. Reddy, S.-Y. Jang, R. A. Segelman, and A. Majumdar, *Science* **315**, 1568 (2007).
- ¹²A. I. Hochbaum, R. K. Chen, R. D. Delgado, W. J. Liang, E. C. Garnett, M. Najarian, A. Majumdar, and P. D. Yang, *Nature (London)* **451**, 163 (2008).
- ¹³S. Lepri, R. Livi, and A. Politi, *Phys. Rep.* **377**, 1 (2003).
- ¹⁴Z. Rieder, J. L. Lebowitz, and E. Lieb, *J. Math. Phys.* **8**, 1073 (1967).
- ¹⁵A. Dhar, *Phys. Rev. Lett.* **86**, 5882 (2001).
- ¹⁶K. Saito, S. Takesue, and S. Miyashita, *Phys. Rev. E* **61**, 2397 (2000).
- ¹⁷D. K. Campbell, P. Rosenau, and G. M. Zaslavsky, *Chaos* **15**, 015101 (2005), and references therein.
- ¹⁸L. Wee Lee and A. Dhar, *Phys. Rev. Lett.* **95**, 094302 (2005).
- ¹⁹H. Zhao, L. Yi, F. Liu, and B. Xu, *Eur. Phys. J. B* **54**, 185 (2006).
- ²⁰D. Barik, *Eur. Phys. J. B* **56**, 229 (2007).
- ²¹D. Segal and A. Nitzan, *Phys. Rev. Lett.* **94**, 034301 (2005); *J. Chem. Phys.* **122**, 194704 (2005).
- ²²D. Segal, *Phys. Rev. B* **73**, 205415 (2006).
- ²³G. E. Uhlenbeck and L. S. Ornstein, *Phys. Rev.* **36**, 823 (1930).
- ²⁴J. Luczka, *Chaos* **15**, 026107 (2005).
- ²⁵S. Lifson and P. S. Stern, *J. Chem. Phys.* **77**, 4542 (1982).
- ²⁶D. Segal, A. Nitzan, and P. Hänggi, *J. Chem. Phys.* **119**, 6840 (2003).
- ²⁷P. Hänggi, *Lect. Notes Phys.* **484**, 15 (1997).
- ²⁸N. W. Ashcroft and N. D. Mermin, *Solid State Physics* (Saunders, Philadelphia, 1976).
- ²⁹R. F. Fox, I. R. Gatland, R. Roy, and G. Vemuri, *Phys. Rev. A* **38**, 5938 (1988).
- ³⁰U. Zürcher and P. Talkner, *Phys. Rev. A* **42**, 3278 (1990).
- ³¹A. Dhar and B. S. Shastry, *Phys. Rev. B* **67**, 195405 (2003).
- ³²M. Terraneo, M. Peyrard, and G. Casati, *Phys. Rev. Lett.* **88**, 094302 (2002).
- ³³J. C. Love, L. A. Estroff, J. K. Kriebel, R. G. Nuzzo, and G. M. Whitesides, *Chem. Rev. (Washington, D.C.)* **105**, 1103 (2005).
- ³⁴J.-D. Bao and Y.-Z. Zhuo, *Phys. Rev. E* **71**, 010102(R) (2005).
- ³⁵X.-P. Zhang and J.-D. Bao, *Phys. Rev. E* **73**, 061103 (2006).
- ³⁶A. Ozpineci and S. Ciraci, *Phys. Rev. B* **63**, 125415 (2001).
- ³⁷N. Mingo, *Phys. Rev. B* **74**, 125402 (2006).
- ³⁸J.-S. Wang, *Phys. Rev. Lett.* **99**, 160601 (2007).
- ³⁹M. Galperin, A. Nitzan, and M. A. Ratner, *Phys. Rev. B* **75**, 155312 (2007).